applied sciences

MDPI

Article

Proposal for a New Bioactive Kinetic Screw in an Implant, Using a Numerical Model

Carlos Aurelio Andreucci [1,*], Abdullah Alshaya [2], Elza M. M. Fonseca [3] and Renato N. Jorge [4]

[1] PhD Engenharia Biomédica, Mechanical Engineering Department, Faculty of Engineering, University of Porto, Rua Dr. Roberto Frias, 712, 4200-465 Porto, Portugal
[2] Mechanical Engineering Department, School of Engineering, College of Petroleum and Engineering, Kuwait University, Fourth Ring Road, Khaldiya, 72301 Kuwait City, Kuwait; abdullah.alshaye@ku.edu.kw
[3] Associated Laboratory for Energy, Transports and Aeronautics (LAETA), Institute of Science and Innovation in Mechanical and Industrial Engineerin (INEGI), Mechanical Engineering Department, School of Engineering, Polytechnic Institute of Porto, R. Dr. António Bernardino de Almeida 431, 4200-072 Porto, Portugal; elz@isep.ipp.pt
[4] Associated Laboratory for Energy, Transports and Aeronautics (LAETA), Institute of Science and Innovation in Mechanical and Industrial Engineerin (INEGI), Mechanical Engineering Department, Faculty of Engineering, University of Porto, Rua Dr. Roberto Frias, 712, 4200-465 Porto, Portugal; rnatal@fe.up.pt
* Correspondence: candreucci@hotmail.com; Tel.: +55-11-983388764

Abstract: A new biomechanism, Bioactive Kinetic Screw (BKS) for screws and bone implants created by the first author, is presented using a bone dental implant screw, in which the bone particles, blood, cells, and protein molecules removed during bone drilling are used as a homogeneous autogenous transplant in the same implant site, aiming to obtain primary and secondary bone stability, simplifying the surgical procedure, and improving the healing process. The new BKS is based on complex geometry. In this work, we describe the growth factor (GF) delivery properties and the in situ optimization of the use of the GF in the fixation of bone screws through a dental implant. To describe the drilling process, an explicit dynamic numerical model was created, where the results show a significant impact of the drilling process on the bone material. The simulation demonstrates that the space occupied by the screw causes stress and deformation in the bone during the perforation and removal of the particulate bone, resulting in the accumulation of material removed within the implant screw, filling the limit hole of the drill grooves present on the new BKS.

Keywords: bone implant contact; growth factors; growth factors delivery; fixation screws; biomechanics

Citation: Andreucci, C.A.; Alshaya, A.; Fonseca, E.M.M.; Jorge, R.N. Proposal for a New Bioactive Kinetic Screw in an Implant, Using a Numerical Model. *Appl. Sci.* **2022**, *12*, 779. https://doi.org/10.3390/app12020779

Academic Editor: Luca Testarelli

Received: 24 November 2021
Accepted: 8 January 2022
Published: 13 January 2022

1. Introduction

Growth factors (GFs) are protein molecules that have a role in controlling biological processes, such as cell growth, proliferation, differentiation, and repair. GFs cannot pass through a cell's membrane; they must bind to high-affinity cell receptors to take effect. Many GFs stimulate several cell populations, while others are less versatile and are specific to a particular cell line. Whatever the tissue involved, the healing process always involves a series of molecular, biochemical, and cellular events that can be grouped into three overlapping phases: inflammation, proliferation, and remodelling [1].

GFs have been used in oral surgery and the most often used and analysed are the bone morphogenetic proteins (BMPs) [2]. More than 20 different BMPs with multiple functions have been detected with an importance in embryogenesis and repair tissues in human adults [3].

Platelet-derived growth factor (PDGF) [1] can be dismissed during blood clotting in any type of tissue injury that promotes chemotaxis and mitogenesis [4].

Fibroblast growth factor (FGF), parathyroid hormone (PTH), transforming growth factor-β (TGF-β), vascular endothelial growth factor (VEGF), and insulin-like growth factor (IGF) have been the subject of various studies [5–13].

Several options have been described [14] to obtain GFs such as autogenous bone grafts, xenografts, allografts, alloplastic grafts, membranes for guided bone regeneration (GBR), platelet-rich plasma (PRP), inlay and onlay grafting, and distraction osteogenesis. Autogenous bone graft is still considered the gold standard for bone repair, despite some difficulties in its application in clinical practice, related to the morbidity of the procedures and the quantity and quality of available bone.

Mixing growth factors with implants or osteo-inductive scaffolds can promote new bone formation at the graft site during replacement of the newly formed bone [1].

The potential of GFs in bone regeneration has been studied by different authors [15–18], but there is no common sense as to how they work together. Further studies are needed to identify predictable in vivo outcomes. The new biomechanism reuses all the material from the cut and perforation performed by the BKS screw as a homogeneous autogenous transplant, stimulating from the beginning of the inflammation the natural healing and repair factors, allowing for better bone remodelling to be tested.

2. Materials and Methods

To describe this ongoing research, an explicit dynamic numerical model was developed using ANSYS 2020 R2 ®—Workbench 2020 R2 with the new BKS biomechanism [19] in titanium alloy versus cortical bone material. This program is a nonlinear transient dynamic finite element program with an explicit time scheme function. The equation of motion is evaluated in the previous time step and works in time step increments, where displacements are calculated as time progresses. Gradually, over time, the deformation also changes. The numerical model aims to simulate the drilling process of the BKS biomechanism and evaluate the mechanical stress distribution in the bone material.

The new BKS biomechanism, as seen in Table 1, also presents itself as a new delivery system for the use of natural growth factors (GF), since the characteristic of the new biomechanism is to introduce protein molecules, cells, blood, and particulate bone through the new screw hole by a drill channel system as an innovative biomechanism; it also becomes a new means of delivery of GFs in surgery for bone expansion, lifting, and fixation [1]. Adding the advantages of using homogeneous autogenous bone (new gold standard to be tested), its macro design is bioactive for the first time in bone implants.

To observe chip formation and chip flow mechanism in a virtual environment, an explicit dynamic finite element analysis must be done with the BKS tool and bone work piece interaction. The BKS diameter is 4 mm and the bone workpiece material has a diameter of 10 mm in diameter, a height of 8 mm, and a central hole of 2 mm with a height of 2 mm.

In this work, three-dimensional finite element modelling, and numerical analysis were carried out to simulate the dynamic process of dental bone perforation. The 3D models were built in Solidworks ®and ANSYS 2020 R2 ®—Workbench 2020 R2 software programs. The BKS modelling was carried out in Solidworks and imported into ANSYS Workbench, as shown in Figure 1. After importing the Solidworks model into ANSYS, a bone block (workpiece) was constructed, representing the surrounding dental bone.

Several authors used the Johnson–Cook model, or its modified formulations [20–25], to investigate and describe problems in which the strain-rate component was relevant. The Johnson–Cook model is the simplest model able to predict the mechanical behaviour of the materials under different loading conditions. It is one of the most used material models, so it is implemented in many finite element codes, and therefore the values of the Johnson–Cook parameters for different materials are quite easy to find in the literature. In the study, both models were modelled by Johnson–Cook material for explicit behaviour, where titanium alloy was chosen as the screw and the workpiece was in bone material. The mechanical properties of the materials used in the study are shown in Table 1.

Figure 1. New biomechanical screw (BKS) of 4 mm width and 10 mm length.

Table 1. Mechanical Properties [23].

	Ti6Al4V of BKS	Bone
Density	4510 kg/m^3	1850 kg/m^3
Shear Modulus	4.4 × 10^{10} Pa	6.54 × 10^8 Pa
Initial Yield Stress	8.5 × 10^8 Pa	1 × 10^7 Pa
Maximum Yield Stress	1.45 × 10^9 Pa	1.25 × 10^8 Pa

Titanium alloys are the most attractive metallic materials for biomedical applications, and are used for various implants and dental devices [26]. Ti6Al4V is heterogeneous and used for different medical implants, namely for dental osseo-integrated screws [26]. The chemical composition of Ti6Al4V is almost 90% titanium, 6.19% aluminium, 3.67% vanadium, 0.17% iron, and 0.12% oxygen [26].

Based on the geometrical models, finite element meshes were generated. The numerical model was prepared in ANSYS 2020 R2 ®—Workbench 2020 R2. The BKS model and the bone disc were meshed with 3D SOLID elements. Lagrangian finite element model-based simulations were performed to determine the effective stress and the effective strain. Different mesh convergence tests were performed to minimize computational error. Figure 2 represents the mesh model and all applied boundary conditions.

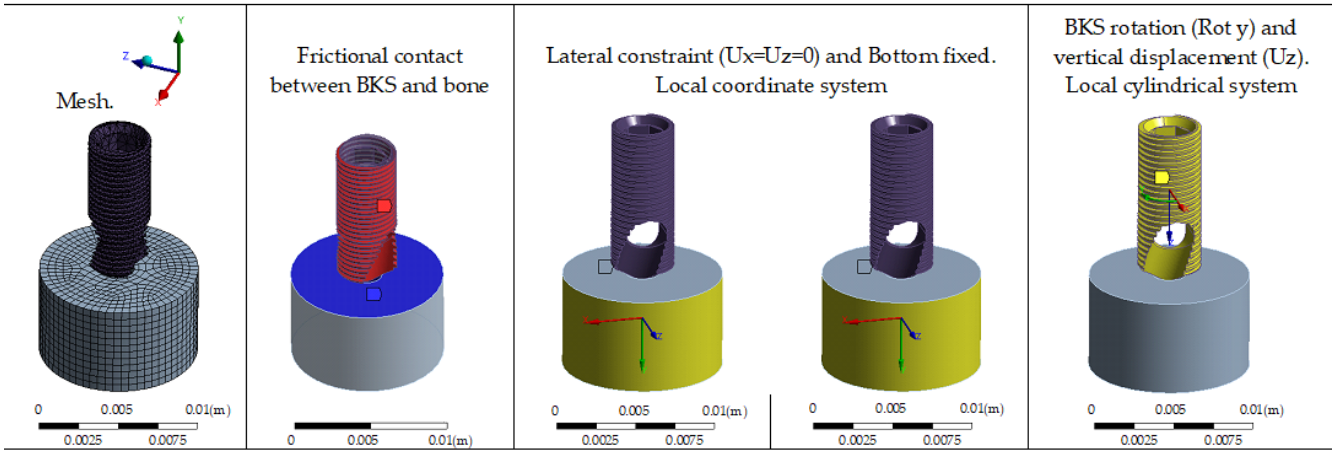

Figure 2. Explicit dynamic analysis: Boundary conditions and mesh.

All boundary conditions were considered due to the dynamic characteristics involved in the drilling process. In the presented simulation, the BKS tool was provided with an angular velocity of 300 rpm and a feed rate equal to 0.5 mm/sec vertically down into the bone, in the absence of irrigation, how it is intended to be used in ongoing research. Only the mechanical load was considered in the model and the thermal effect produced by the BKS was not considered in the present simulation.

In the simulation, the end time specifies the number of iterations to be performed by the solver and informs the solver when to stop the process. Since the bone workpiece is 8 mm in length, and the feed rate is 0.5 mm/s, then a final time of 16 s is needed for the entire length of the screw to be covered with the bone. The contact between the BKS-cortical bone is designed to be frictional, with a static friction coefficient equal to 0.4 and a dynamic friction coefficient 0.2. The bottom and the lateral face of the bone workpiece were fixed, with free movement in the axial direction, as shown in Figure 2.

The numerical model consisted of a total of 17,079 linear elements (BKS with tetrahedrons and bone in hexahedron elements) with a total of 9588 nodes. The element size used in the bone was equal to 5×10^{-4} m. The BKS was analysed under dynamic loading to ensure the safety of the design. The loading step type was the explicit integration of time into final time equal to 6×10^{-4} s. The contact interaction was formulated using the algorithm proposed from the program. The contact surface is updated as elements on the free surface are deleted according to the material's failure criteria. In this work, erosion controls with geometric strain limit were imposed equal to 1.5 on material criteria failure.

3. Results and Discussion

Numerical results of strain and stress level were obtained during the drilling process. Figure 3 shows the numerical results of strain and stress at the end of the simulation.

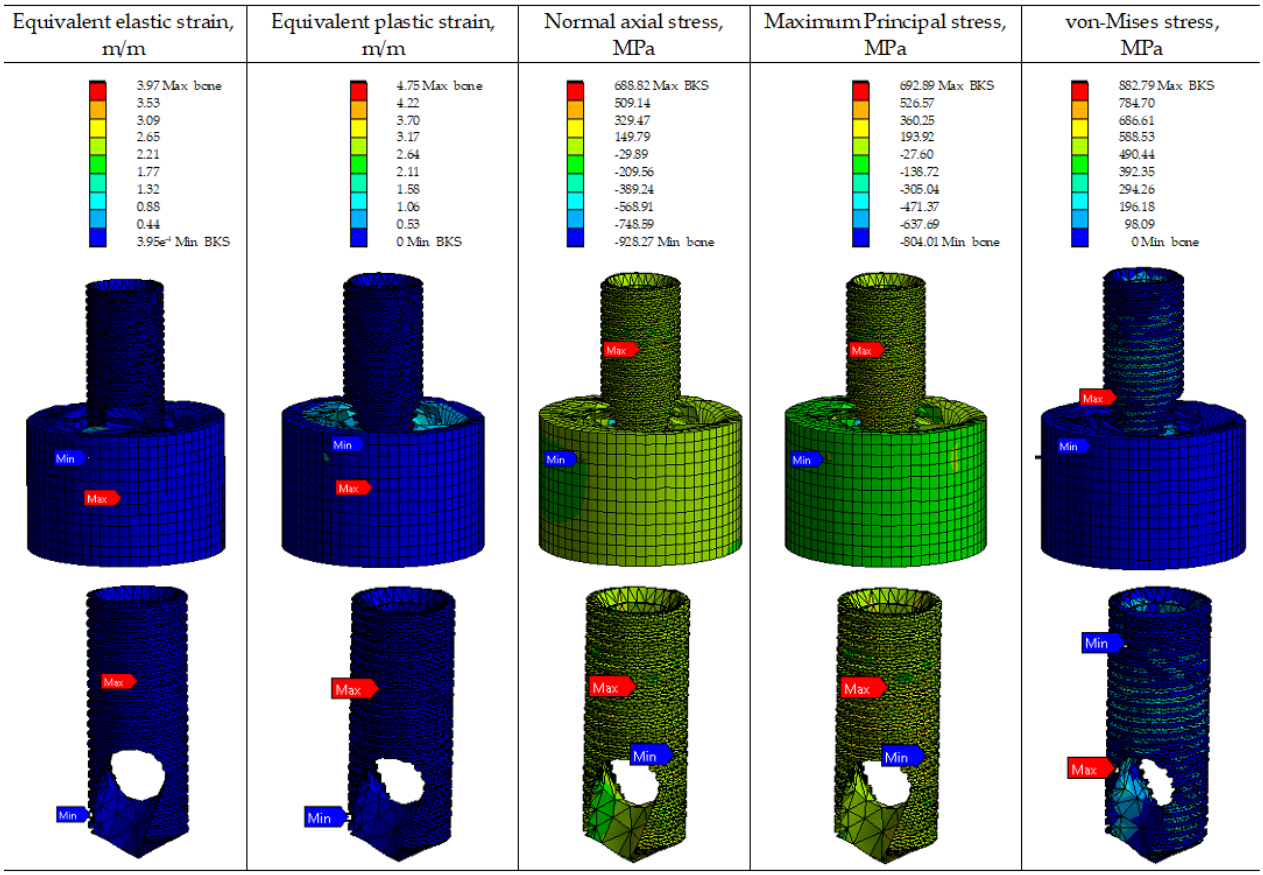

Figure 3. Numerical results at the end time of the simulation.

The numerical results show a significant impact of the drilling process on the bone material at the end of the simulation, with a higher level of strain and stress.

The numerical results show that the stress and strain level in the bone tends to increase with the perforation of BKS. In the depth of the hole around the centre of the material, the BKS exerted greater stress and strain, consequently causing more deformation.

The equivalent elastic strain determines the variation in the stress impact of the drilling process on the material. Extreme strain was induced at the edge of the material, inside the central hole of the bone.

The equivalent stress value is higher when compared to the yield stress material. After the stresses beyond the yield point, the material undergoes inelastic strain and a permanent deformation occurs, called plastic deformation. The equivalent plastic strain is the total strain energy of this plastic deformation.

Figure 4 shows the formation of the plastic strain over different time instants of the drilling process. Different images were collected from which it is possible to identify that the BKS screw during the drilling process does not present plastic strain. Bone material during perforation presents high plastic strain which increases with the material removed.

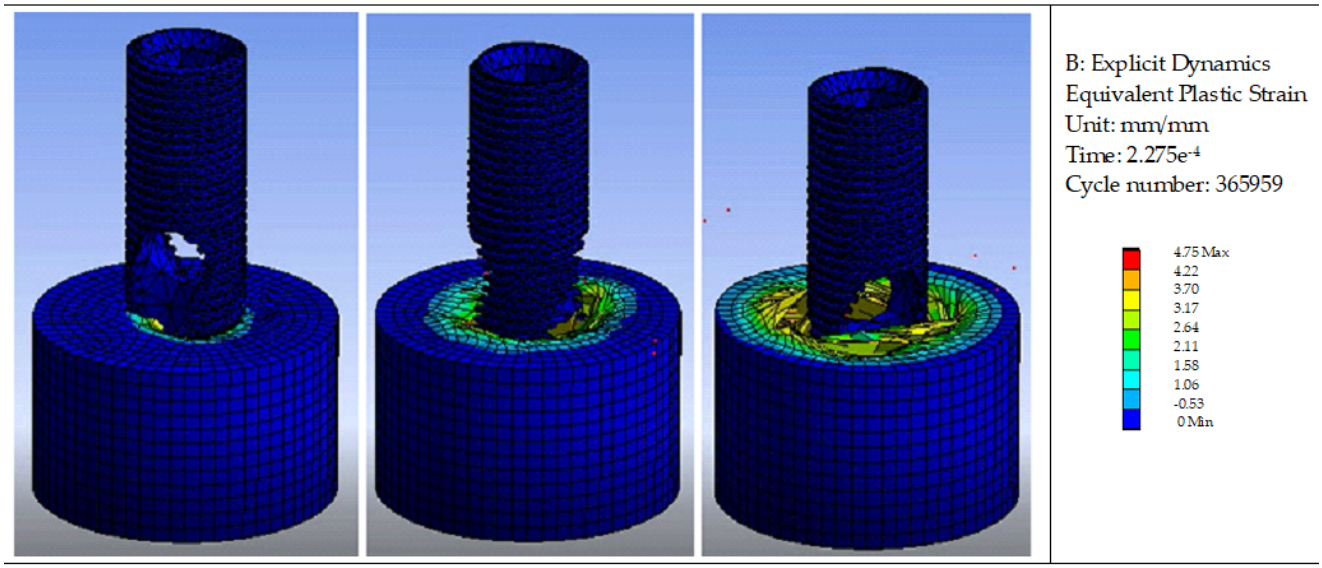

Figure 4. Numerical results of the plastic strain at different time instants.

The surface around the drilled hole demonstrated the high strain at the beginning of the drilling operation. In the drilled hole, it could be verified that the elements were removed when the yield stress and rupture due to plastic strain in the material were reached.

The simulation described demonstrates that the space occupied by the screw causes stress and deformation in the bone during the perforation and removal of the bone particle, resulting in the accumulation of material removed inside the implant screw filling the limit hole of the drill grooves present in the new biomechanism. This material was released during the surgical bone drilling, along with the bone particle created in the drilling step.

New Line of Research for Osseo-Integrated Screws

Bone regeneration using implants coated with GFs stimulated local osseo-integration using screw-type dental implants [18].

The great potential of GFs in bone regeneration has been discussed by several authors [15–18], their limitations seem to be the unpredictable nature of the resulting tissue regeneration in vivo [27].

Giannoudis et al. [28] introduced the "Diamond Concept" to describe the conditions necessary for osteogeneration: mechanical stability at the defect site, osteogenic cells combined with osteo-inductive growth factors, and a suitable carrier or delivery system.

The delivery system ensures normal protein concentrations at the site of injury for as long as necessary to allow the regenerative cells to migrate, proliferate, and differentiate [29,30].

Collagen is the most abundant protein in the mammalian connective tissue and the main non-mineral component of bone. It has been prepared in implantable absorbable powders, membranes, films, and sponges, as well as in aqueous forms. Although versatile and easy to manipulate, the manufacture of collagen carriers is highly sensitive to several factors (including mass, soak time, protein concentration, sterilization, buffer composition, pH, and ionic strength) that directly affect rhBMPs binding [31].

Alginate is a non-immunogenic polysaccharide used in a wide range of tissue engineering applications for its gel-forming properties. Alginate hydrogels, allowing a controlled and prolonged release of BMPs, have been studied only in the preclinical phase, with promising results in vitro [32,33]. Chitosan is a cationic gluco-polymer well known for its biological, chelating, and adsorbent properties, and has been used as a BMP-2 carrier in a rat critical-size mandibular defect model, with positive results in histological and histomorphometric analyses [34]. Hyaluronic acid is a naturally occurring biopolymer that plays a significant role in wound healing. It has been associated with improved bone formation in mandibular defects compared to collagen sponges when both were used to carry rhBMP-2 [35].

Hydroxyapatite (HA) has been widely used as a bone substitute material in clinical practice since the 1970s due to its ability to bind directly to bone [6,33,36–38]. The most used polymers applied as bone grafts are polylactic acid (PLLA) and polyglycolic acid (PLGA) [39].

Bone grafts act as scaffolds, allowing bone to grow on their surface and into the material. The combination of osteoconductive scaffolds with osteo-inductive proteins has been a major focus of research [40,41]. The coating GFs on dental implant surfaces have been shown to be able to stimulate bone formation around the implants [28,42]. Some research with gene delivery through adenoviral or liposomal vectors in animal models have been studied [43,44].

Scarano et al. [45] studying bone formation in the concavities and convexities of dental implants, demonstrated that early bone formation was observed mainly in the concavities of implant screws inserted in rabbit tibia. Among other factors, there was a greater concentration of vessels within these concavities. The experiment results supported this hypothesis and the formation of blood vessels appeared to be stimulated by the presence of Scoops.

Platelet-rich fibrin (PRF) [46] is an autologous material that is easy to produce; it can be derived from a person's own blood and is used to promote wound healing and tissue regeneration. PRF is expected to have a direct effect on enhancing tissue regeneration by saturating these tissues with blood growth factors. This is especially important in tissues with limited blood supply, such as bone tissue compared to soft tissue.

In the new biomechanism (BKS) the hard tissue removed during bone drilling and screwing at the same time, due to the new characteristics, uses the chips (bone particles, blood, cells, and protein molecules) to fill the hole passing through the drill grooves in the new screw. The screw was created based on the concepts of using drills for bone drilling and screws for fixing and implants [41]. Considering that the traditional drill flutes eliminate the bone particulate removed after cutting, the author created a limit for these flutes that are found through a hole connecting and limiting the cut grooves, preventing the removal of all material from the drilling. This drilling particulate material is compacted in and through the screw, increasing the bone contact surface and creating a graft bone bridge of particulate material through the screw.

With surface treatments using electrochemical anodization [47] to create nanotubes and the coating with (CaP), [48] we can make the new screw, bioactive model in macro-, micro-, and nano-design, and the delivery system "diamond concept" [28] of GFs in a new biomechanism which meets the characteristics that are still considered the gold standard [1] for bone healing in implants and fixations screws. Future studies will aim to confirm these

results for this new biomechanism. Furthermore, a new line of research is opened up for osseo-integrated screws, with homogenous autogenous transplant and a growth factor delivery system.

4. Conclusions

The proposed new Bioactive Kinetic Screw (BKS) allows the use of bone, blood, cells, and protein molecules removed in bone drilling to be introduced through the screw using an innovative insertion and compacting biomechanism. This makes it a new growth factor delivery system to be tested, where all the stages in which these factors act, inflammation, proliferation, and remodelling are attended to, as well as the principles of the gold standard for autogenous transplantation and the diamond concept for delivery system being retained. The immediate use of homogeneous autogenous bone, blood, protein molecules, and cells without external manipulation to deliver GFs is innovative, creating new possibilities for both research and studies in bone healing, fracture fixation, bone implants, and osseo-integration. This work also presents the stresses generated during bone drilling using the dynamic explicit finite element method. This numerical model provides a new and enhanced approach to dental bone drilling based on the complex geometry of the new BKS. As a general conclusion, the stress level increases with drilling time and with increasing hole depth. These numerical models can be used as an important tool for planning accurate and safe medical procedures. In the present study, there is a limitation in the numerical model. Only the mechanical load was considered in the model and not the thermal effect produced by the BKS. Future work will involve the thermo–mechanical process to compare the results with the present research.

Author Contributions: Conceptualization, C.A.A.; methodology, C.A.A.; validation, C.A.A. and A.A.; investigation, C.A.A. and A.A.; writing—original draft preparation, C.A.A. and E.M.M.F.; writing—review and editing, E.M.M.F. and R.N.J.; supervision, R.N.J. All authors have read and agreed to the published version of the manuscript.

Funding: This research received no external funding.

Institutional Review Board Statement: Not applicable.

Informed Consent Statement: Not applicable.

Data Availability Statement: Not applicable.

Conflicts of Interest: The authors declare no conflict of interest.

References

1. Sivolella, S.; De Biagi, M.; Brunello, G.; Ricci, S.; Tadic, D.; Marinc, C.; Lops, D.; Ferroni, L.; Gardin, C.; Bressan, E.; et al. Delivery Systems and Role of Growth Factors for Alveolar Bone Regeneration in Dentistry. In *Book Regenerative Medicine and Tissue Engineering*; Jose, A.A., Ed.; IntechOpen: London, UK, 2013.
2. Urist, M.R. Bone: Formation by autoinduction. *Science* **1965**, *150*, 893–899. [CrossRef] [PubMed]
3. Bragdon, B.; Moseychuk, O.; Saldanha, S.; King, D.; Julian, J.; Nohe, A. Bone Morphogenetic Proteins: A critical review. *Cell Signal.* **2011**, *23*, 609–620. [CrossRef] [PubMed]
4. Kaigler, D.; Avila, G.; Wisner-Lynch, L.; Nevins, M.L.; Nevins, M.; Rasperini, G.; Lynch, S.E.; Giannobile, W.V. Platelet-derived growth factor applications in periodontal and peri implant bone regeneration. *Expert Opin. Biol. Ther.* **2011**, *11*, 375–385. [CrossRef]
5. Bizenjima, T.; Seshima, F.; Ishizuka, Y.; Takeuchi, T.; Kinumatsu, T.; Saito, A. Fibroblast growth factor-2 promotes healing of surgically created periodontal defects in rats with early, streptozotocin-induced diabetes via increasing cell proliferation and regulating angiogenesis. *J. Clin. Periodontol.* **2015**, *42*, 62–71. [CrossRef]
6. Benington, L.; Rajan, G.; Locher, C.; Lim, L.Y. Fibroblast Growth Factor 2-A Review of Stabilisation Approaches for Clinical Applications. *Pharmaceutics* **2020**, *12*, 508. [CrossRef]
7. Behr, B.; Sorkin, M.; Lehnhardt, M.; Renda, A.; Longaker, M.T.; Quarto, N. A Comparative Analysis of the Osteogenic Effects of BMP-2, FGF-2, and VEGFA in a Calvarial Defect Model. *Tissue Eng. Part A* **2012**, *18*, 1079–1086. [CrossRef]
8. Chen, G.; Deng, C.; Li, Y.-P. TGF-β and BMP Signaling in Osteoblast Differentiation and Bone Formation. *Int. J. Biol. Sci.* **2012**, *8*, 272–288. [CrossRef]
9. Jung, R.E.; Thoma, D.S.; Hammerle, C.H. Assessment of the potential of growth factors for localized alveolar ridge augmentation: A systematic review. *J. Clin. Periodontol.* **2008**, *35* (Suppl. S8), 255–281. [CrossRef]

10. Palioto, D.B.; Rodrigues, T.L.; Marchesan, J.T.; Beloti, M.M.; de Oliveira, P.T.; Rosa, A.L. Effects of enamel matrix derivative and transforming growth factor-β1 on human osteoblastic cells. *Head Face Med.* **2011**, *7*, 13. [CrossRef]
11. Teare, J.A.; Petit, J.C.; Ripamonti, U. Synergistic induction of periodontal tissue regeneration by binary application of human osteogenic protein-1 and human transforming growth factor-β(3) in Class II furcation defects of Papio ursinus. *J. Periodontal. Res.* **2012**, *47*, 336–344. [CrossRef] [PubMed]
12. Oliveira, É.R.; Nie, L.; Podstawczyk, D.; Allahbakhsh, A.; Ratnayake, J.; Brasil, D.L.; Shavandi, A. Advances in Growth Factor Delivery for Bone Tissue Engineering. *Int. J. Mol. Sci.* **2021**, *22*, 903. [CrossRef] [PubMed]
13. Lossdörfer, S.; Abuduwali, N.; Jäger, A. Bone morphogenetic protein-7 modifies the effects of insulin-like growth factors and intermittent parathyroid hormone (1-34) on human periodontal ligament cell physiology in vitro. *J. Periodontol.* **2011**, *82*, 900–908. [CrossRef] [PubMed]
14. Esposito, M.; Grusovin, M.G.; Felice, P.; Karatzopoulos, G.; Worthington, H.V.; Coulthard, P. Interventions for replacing missing teeth: Horizontal and vertical bone augmentation techniques for dental implant treatment. *Cochrane Database Syst. Rev.* **2009**, *4*, CD003607. [CrossRef] [PubMed]
15. Bessa, P.C.; Casal, M.; Reis, R.L. Bone morphogenetic proteins in tissue engineering: The road from the laboratory to the clinic, part I (basic concepts). *J. Tissue Eng. Regen. Med.* **2008**, *2*, 1–13. [CrossRef]
16. Kao, D.W.; Fiorellini, J.P. Regenerative periodontal therapy. *Front. Oral. Biol.* **2012**, *15*, 149–159. [PubMed]
17. Park, J.B. Use of bone morphogenetic proteins in sinus augmentation procedure. *J. Craniofac. Surg.* **2009**, *20*, 1501–1503. [CrossRef]
18. Wikesjö, U.M.; Qahash, M.; Huang, Y.H.; Xiropaidis, A.; Polimeni, G.; Susin, C. Bone morphogenetic proteins for periodontal and alveolar indications; biological observations—Clinical implications. *Orthod. Craniofac. Res.* **2009**, *12*, 263–270. [CrossRef] [PubMed]
19. Andreucci, C.A.; Fonseca, E.M.M.; Jorge, R.N. *Advances and Current Trends in Biomechanics*, 1st ed.; Taylor & Francis: London, UK, 2021; pp. 1–4.
20. Khare, S.; Kumar, K.; Choudhary, S.; Singh, P.K.; Verma, R.K.; Mahajan, P. Determination of Johnson–Cook Material Parameters for Armour Plate Using DIC and FEM. *Met. Mater. Int.* **2021**, *27*, 4984–4995. [CrossRef]
21. Fernandes, M.G.; Fonseca, E.M.M.; Natal, R.; Manzanares, M.C. Ex vivo experimental and numerical study of stresses distribution in human cadaveric tibiae. *Int. J. Med. Eng. Inform.* **2021**, *13*, 164–173. [CrossRef]
22. Steinberg, D.J. Equation of State and Strength Properties of Selected Materials—Lawrence Livermore National Laboratory Report UCRL-MA-106439. 1991. Available online: https://xs2.dailyheadlines.cc/scholar?q=Equation+of+State+and+Strength+Properties+of+Selected+Materials+-+Lawrence+Livermore+National+Laboratory+report+UCRL-MA-106439 (accessed on 24 July 2021).
23. Fernandes, M.G.; Fonseca, E.M.; Natal, R.M. Three-dimensional dynamic finite element and experimental models for drilling processes. *Proc IMechE Part L J. Mater. Design Appl.* **2015**, *232*, 35–43. [CrossRef]
24. Fernandes, M.G.; Fonseca, E.M.M.; Natal, R. Thermo-mechanical stresses distribution on bone drilling: Numerical and experimental procedures. *Proc. Inst. Mech. Eng. Part L J. Mater. Design Appl.* **2019**, *233*, 637–646. [CrossRef]
25. Fernandes, M.G.; Fonseca, E.M.M.; Natal, R.; Dias, M.I.R. Thermal analysis in drilling of ex vivo bovine bones. *J. Mech. Med. Biol.* **2017**, *17*, 1–16. [CrossRef]
26. Zatkalíková, V.; Palček, P.; Markovičová, L.; Chalupová, M. Analysis of fractured screw shaped Ti6Al4V dental implant. *Mater. Today Proc. 3* **2016**, 1216–1219. [CrossRef]
27. Dard, M.; Sewing, A.; Meyer, J.; Verrier, S.; Roessler, S.; Scharnweber, D. Tools for tissue engineering of mineralized oral structures. *Clin. Oral. Invest.* **2000**, *4*, 126–129. [CrossRef] [PubMed]
28. Giannoudis, P.V.; Psarakis, S.; Kanakaris, N.K.; Pape, H.C. Biological enhancement of bone healing with Bone Morphogenetic Protein-7 at the clinical setting of pelvic girdle non-unions. *Injury* **2007**, *38*, S43–S48. [CrossRef]
29. Haidar, Z.S.; Hamdy, R.C.; Tabrizian, M. Delivery of recombinant bone morphogenetic proteins for bone regeneration and repair. *Part A Curr. Chall. BMP Deliv. Biotechnol. Lett.* **2009**, *31*, 1817–1824.
30. Benglis, D.; Wang, M.Y.; Levi, A.D. A comprehensive review of the safety profile of bone morphogenetic protein in spine surgery. *Neurosurgery* **2008**, *62*, ONS423–ONS431.
31. Haidar, Z.S.; Hamdy, R.C.; Tabrizian, M. Delivery of recombinant bone morphogenetic proteins for bone regeneration and repair. Part B: Delivery systems for BMPs in orthopaedic and craniofacial tissue engineering. *Biotechnol. Lett.* **2009**, *31*, 1825–1835. [CrossRef]
32. Jeon, O.; Song, S.J.; Yang, H.S.; Bhang, S.H.; Kang, S.W.; Sung, M.A.; Lee, J.H.; Kim, B.S. Long term delivery enhances in vivo osteogenic efficacy of bone morphogenetic protein-2 740 Regenerative Medicine and Tissue Engineering compared to short-term delivery. *Biochem. Biophys. Res. Commun.* **2008**, *369*, 774–780. [CrossRef]
33. Lim, S.M.; Oh, S.H.; Lee, H.H.; Yuk, S.H.; Im, G.I.; Lee, J.H. Dual growth factor-releasing nano- particle/hydrogel system for cartilage tissue engineering. *J. Mater. Sci. Mat. Med.* **2010**, *21*, 2593–2600. [CrossRef]
34. Issa, J.P.; Bentley, M.V.; Iyomasa, M.M.; Sebald, W.; De Albuquerque, R.F. Sustained release carriers used to delivery bone morphogenetic proteins in the bone healing process. *Anat. Histol. Embryol.* **2008**, *37*, 181–187. [CrossRef] [PubMed]
35. Arosarena, O.A.; Collins, W.L. Bone regeneration in the rat mandible with bone morphogenetic protein-2: A comparison of two carriers. *Otolaryngol. Head. Neck. Surg.* **2005**, *132*, 592–597. [CrossRef]
36. Li, R.H.; Wozney, J.M. Delivering on the promise of bone morphogenetic proteins. *Trends. Biotechnol.* **2001**, *19*, 255–265. [CrossRef]

37. Kim, S.S.; Gwak, S.J.; Kim, B.S. Orthotopic bone formation by implantation of apatite coated poly(lactide-co-glycolide)/hydroxyapatite composite particulates and bone morphogenetic protein-2. *J. Biomed. Mater. Res.* **2008**, *87*, 245–253. [CrossRef]
38. Schopper, C.; Moser, D.; Spassova, E.; Goriwoda, W.; Lagogiannis, G.; Hoering, B.; Ewers, R.; Redl, H. Bone re generation using a naturally grown HA/TCP carrier loaded with rh BMP-2 is independent of barrier-membrane effects. *J. Biomed. Mater. Res.* **2008**, *85*, 954–963. [CrossRef]
39. Zellin, G.; Linde, A. Importance of delivery systems for growth-stimulatory factors in combination with osteopromotive membranes. An experimental study using rhBMP-2 in rat mandibular defects. *J. Biomed. Mater. Res.* **1997**, *35*, 181–190. [CrossRef]
40. Gruber, R.M.; Ludwig, A.; Merten, H.A.; Pippig, S.; Kramer, F.J.; Schliephake, H. Sinus floor augmentation with recombinant human growth and differentiation factor-5 (rhGDF-5): A pilot study in the Goettingen miniature pig comparing autogenous bone and rhGDF-5. *Clin. Oral. Implants Res.* **2009**, *20*, 175–182. [CrossRef]
41. Albrektsson, T.; Johansson, C. Osteoinduction, osteoconduction and osseointegration. *Eur. Spine J.* **2001**, *10* (Suppl. S2), S96–S101.
42. Liu, Y.; Enggist, L.; Kuffer, A.F.; Buser, D.; Hunziker, E.B. The influence of BMP-2 and its mode of delivery on the osteoconductivity of implant surfaces during the early phase of osseointegration. *Biomaterials* **2007**, *28*, 2677–2686. [CrossRef]
43. Lutz, R.; Park, J.; Felszeghy, E.; Wiltfang, J.; Nkenke, E.; Schlegel, K.A. Bone regeneration after topical BMP-2-gene delivery in circumferential peri-implant bone defects. *Clin. Oral. Implants Res.* **2008**, *19*, 590–599. [CrossRef]
44. Chang, S.C.; Lin, T.M.; Chung, H.Y.; Chen, P.K.; Lin, F.H.; Lou, J.; Jeng, L.B. Large-scale bicortical skull bone regeneration using ex vivo replication-defective adenoviral-mediated bone morphogenetic protein-2 gene-transferred bone marrow stromal cells and composite biomaterials. *Neurosurgery* **2009**, *65* (Suppl. S6), 75–81. [CrossRef]
45. Scarano, A.; Perrotti, V.; Artese, L.; Degidi, M.; Degidi, D.; Piattelli, A.; Iezzi, G. Blood vessels are concentrated within the implant surface concavities: A histologic study in rabbit tibia. *Odontology* **2014**, *102*, 259–266. [CrossRef] [PubMed]
46. Egle, K.; Salma, I.; Dubnika, A. From Blood to Regenerative Tissue: How Autologous Platelet-Rich Fibrin Can Be Combined with Other Materials to Ensure Controlled Drug and Growth Factor Release. *Int. J. Mol. Sci.* **2021**, *22*, 11553. [CrossRef] [PubMed]
47. Galstyan, V.; Comini, E.; Faglia, G.; Sberveglieri, G. TiO2 Nanotubes: Recent Advances in Synthesis and Gas Sensing Properties. *Sensors* **2013**, *13*, 14813–14838. [CrossRef] [PubMed]
48. Su, B.; Peng, X.; Jiang, D.; Wu, J.; Qiao, B.; Li, W.; Qi, X. In Vitro and In Vivo Evaluations of Nano-Hydroxyapatite/Polyamide 66/Glass Fiber (n-HA/PA66/GF) as a Novel Bioactive Bone Screw. *PLoS ONE* **2013**, *8*, e68342. [CrossRef] [PubMed]